Supplementary Materials for

Tissue-resident PSGL1^{lo}CD4^{+} T cells promote B cell differentiation and chronic graft-versus-host-disease-associated autoimmunity

Xiaohui Kong[1, 2*], Deye Zeng[1, 2,3*], Xiwei Wu[4], Bixin Wang[1,2, 5], Shijie Yang[1,2,6], Qingxiao Song[1, 2, 5], Yongping Zhu[1, 2], Martha Salas[1, 2], Hanjun Qin[4], Ubaydah Nasri[1, 2], Karen M. Haas[7], Arthur D. Riggs[1], Ryotaro Nakamura[2], Paul J. Martin[8], Aimin Huang[3$], and Defu Zeng[1, 2$]

$ Corresponding authors: Dr. Defu Zeng, The Beckman Research Institute of City of Hope; email dzeng@coh.org. or Dr. Aimin Huang, Fujian Medical University, China; email: draimin@163.com

Files include Supplemental Figures and Tables as well as supplemental materials and methods.

I. Supplemental Figures and Tables

II. Supplemental Materials and Methods

I. Supplemental Figures and Tables

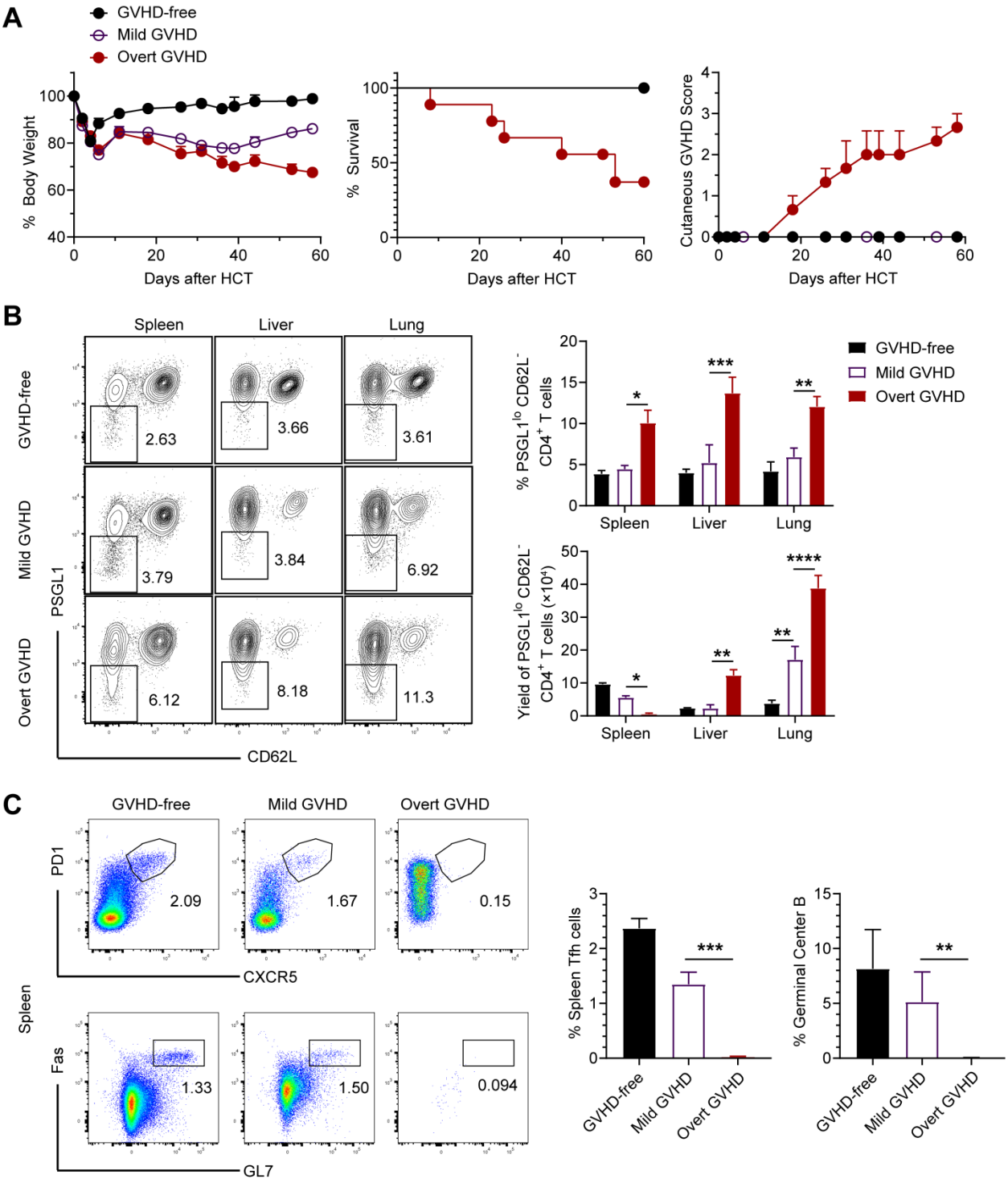

Supplemental Figure 1

Supplemental Figure 1. PSGL1^{lo}CD4^{+} T cell expansion was associated with GC destruction and cGVHD severity. WT BALB/c recipients were given TCD-BM alone or with 0.1M and 1.0M splenocytes. Recipients were monitored for GVHD development and tissues were harvested at 60 days after HCT. **(A)** Curves of % Body weight changes, % survivor and Cutaneous GVHD score. **(B)** Representative flow cytometry patterns, percentage and yield of donor type H2Kb^{+}PSGL1^{lo}CD62L^{-}CD4^{+}TCRβ^{+} T cells are shown as means ± SEM. **(C)** Representative flow cytometry patterns and percentage of spleen Tfh cells and GC B cells are shown. N=6 from 2 replicate experiments. P values were calculated by two-way ANOVA **(B)** and one-way ANOVA **(C)**. *p<0.05; **p<0.01; ***p<0.001; ****p<0.0001.

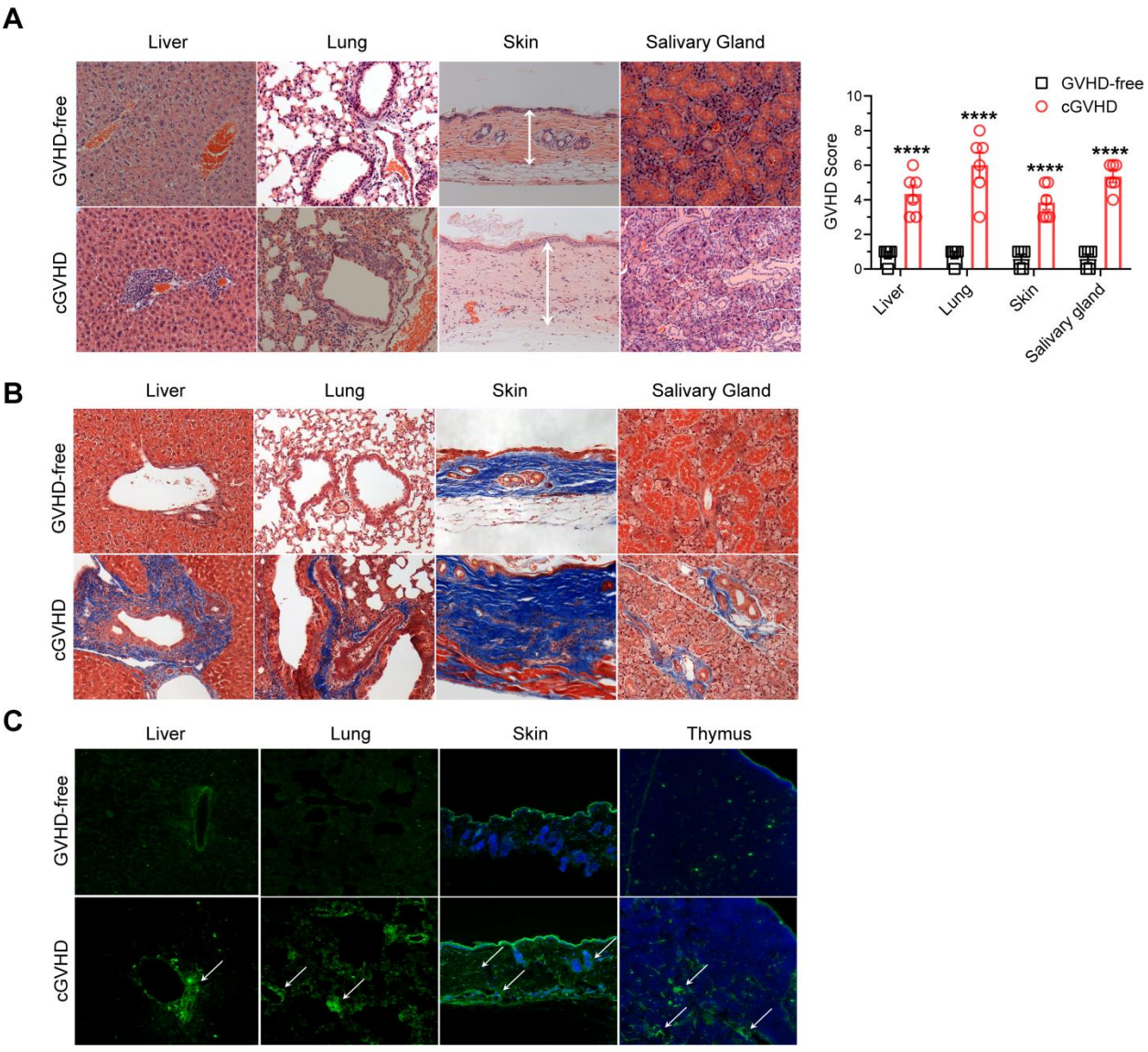

Supplemental Figure 2

Supplemental Figure 2. Pathology, Fibrosis and autoantibody deposition in cGVHD target tissues. This is a supplement to Figure 1. cGVHD was induced as described in Figure 1. The results compare GVHD-free and cGVHD recipients. **(A)** HE staining of liver, lung, skin and salivary gland of GVHD-free and cGVHD mice, pathology scores are also shown (original magnification, ×200). **(B)** Trichrome staining of liver, lung, skin and salivary gland tissues (original magnification, ×200). **(C)** IgG autoantibody deposition in the liver, lung, skin and thymus (original magnification, ×200). White arrows show IgG deposition. N=6, combined from 2 independent experiments. Data present means±SEM. P values were calculated by one-way ANOVA **(A)**. ****, $p<0.0001$.

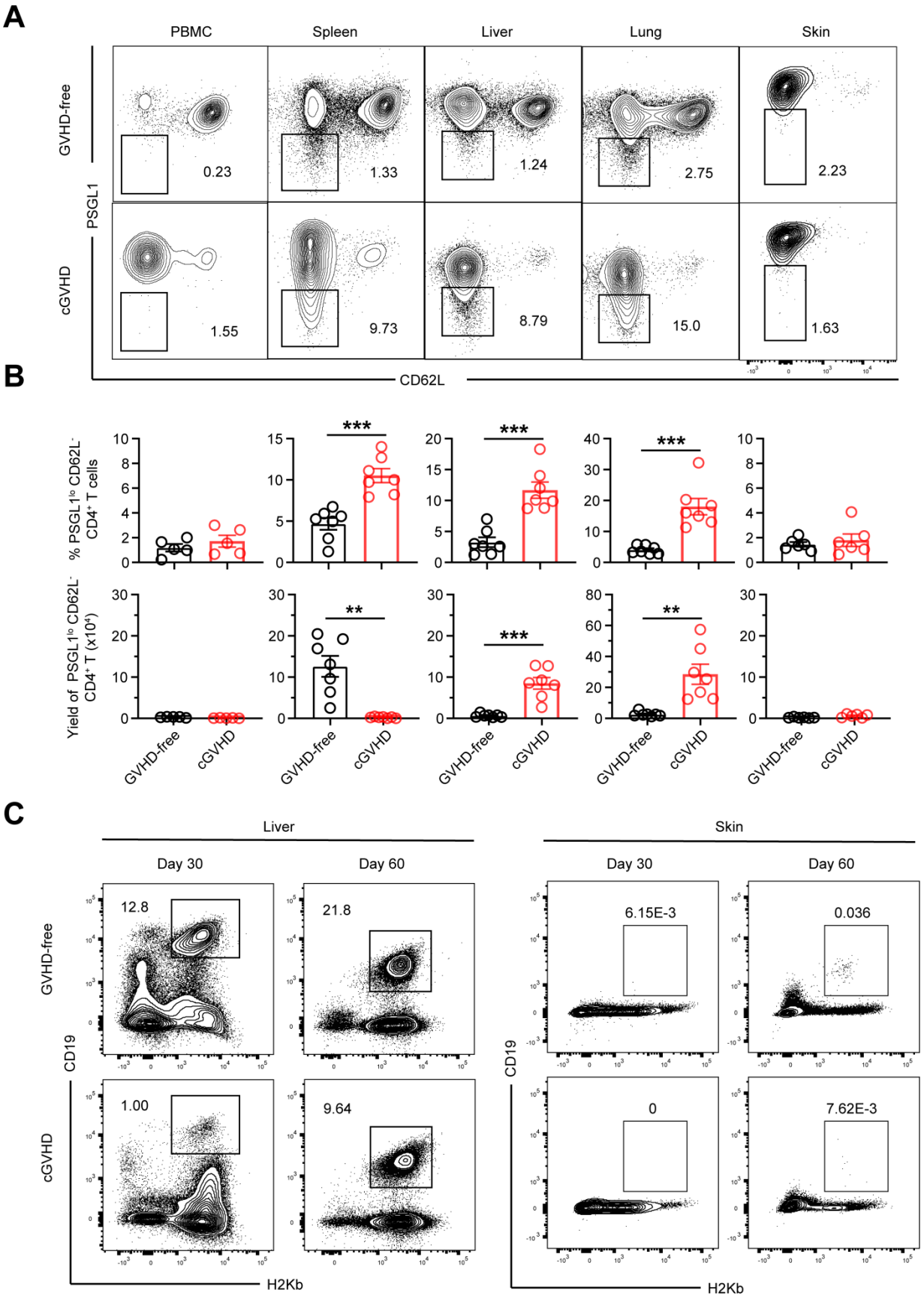

Supplemental Figure 3

Supplemental Figure 3: PSGL1^{lo}CD4^{+} T cells are not detectable in the blood or skin, and B cells are not detectable in the skin. HCT was performed as described in Figure 1. **(A & B),** 30 days after HCT, the percentage and yield of PSGL1^{lo}CD4^{+} T cells in the blood, spleen, liver, lung and skin were analyzed with flow cytometry. Representative flow cytometry patterns and mean ± SEM are shown. N=5-8 combined from three replicate experiments. **(C)** CD19^{+} B cells in the liver and skin of GVHD-free and GVHD recipients at 30 and 60 days after HCT. Representative flow cytometry patterns are shown. 4 recipients in each group combined from two replicate experiments. P values were calculated by unpaired 2-tailed Student's t-tests. *p<0.05; **p<0.01; ***p<0.001; ****p<0.0001.

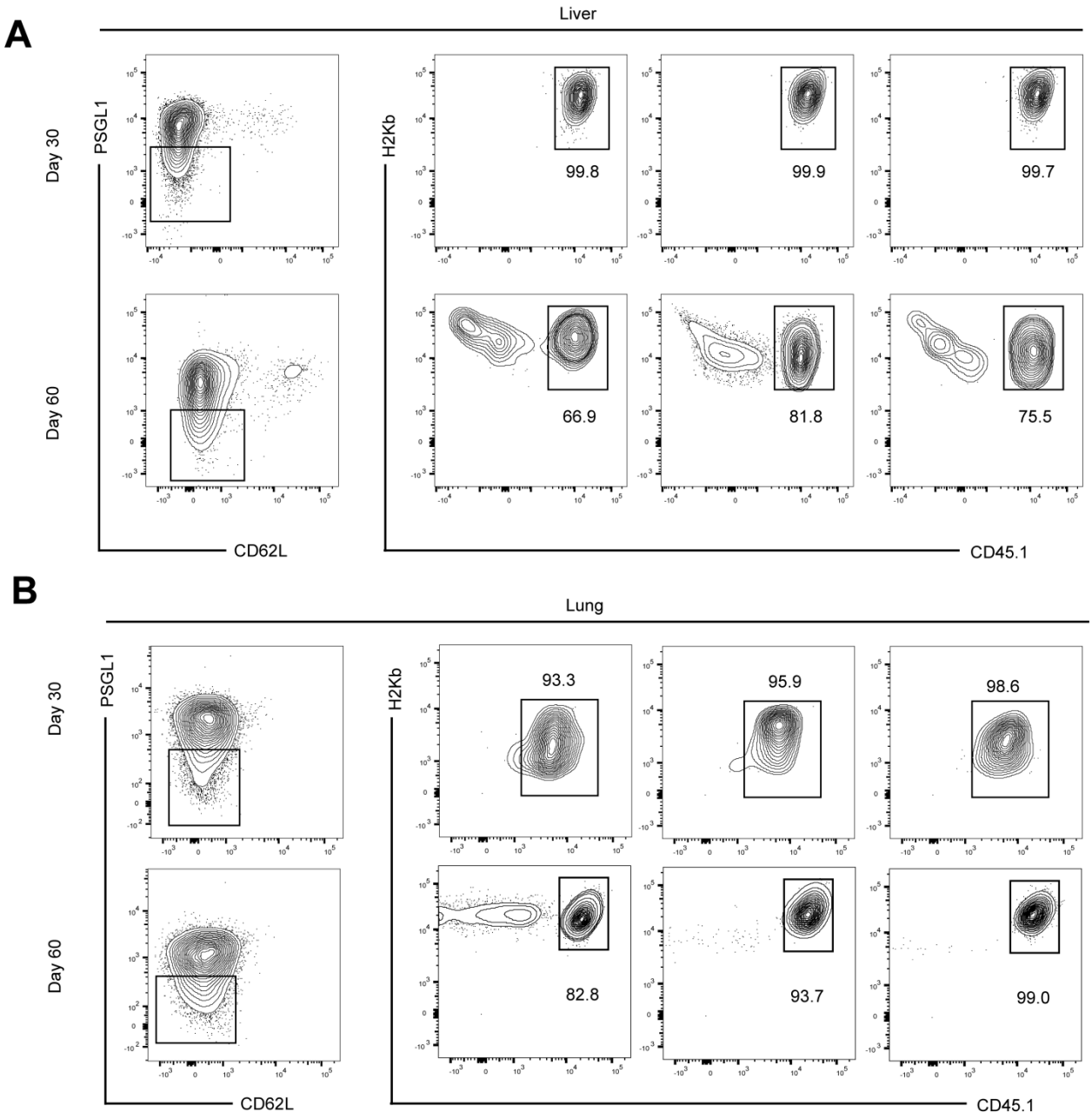

Supplemental Figure 4

Supplemental Figure 4: PSGL1^{lo}CD4^{+} T cells are mainly derived from the injected donor T cells. Lethally irradiated BALB/c mice received CD45.2^{+} TCD-BM cells and congenic CD45.1^{+} T cells. Recipients developed cGVHD. 30 and 60 days after HCT, donor-type PSGL1^{lo}CD62L^{-} CD4^{+} T cells from the liver **(A)** and lung **(B)** are identified with CD45.1 and H-2K^{b} staining. The injected H-2K^{b}CD45.1^{+} T cells are boxed. Representative flow cytometry patterns are shown from 1 of 3 replicate experiments.

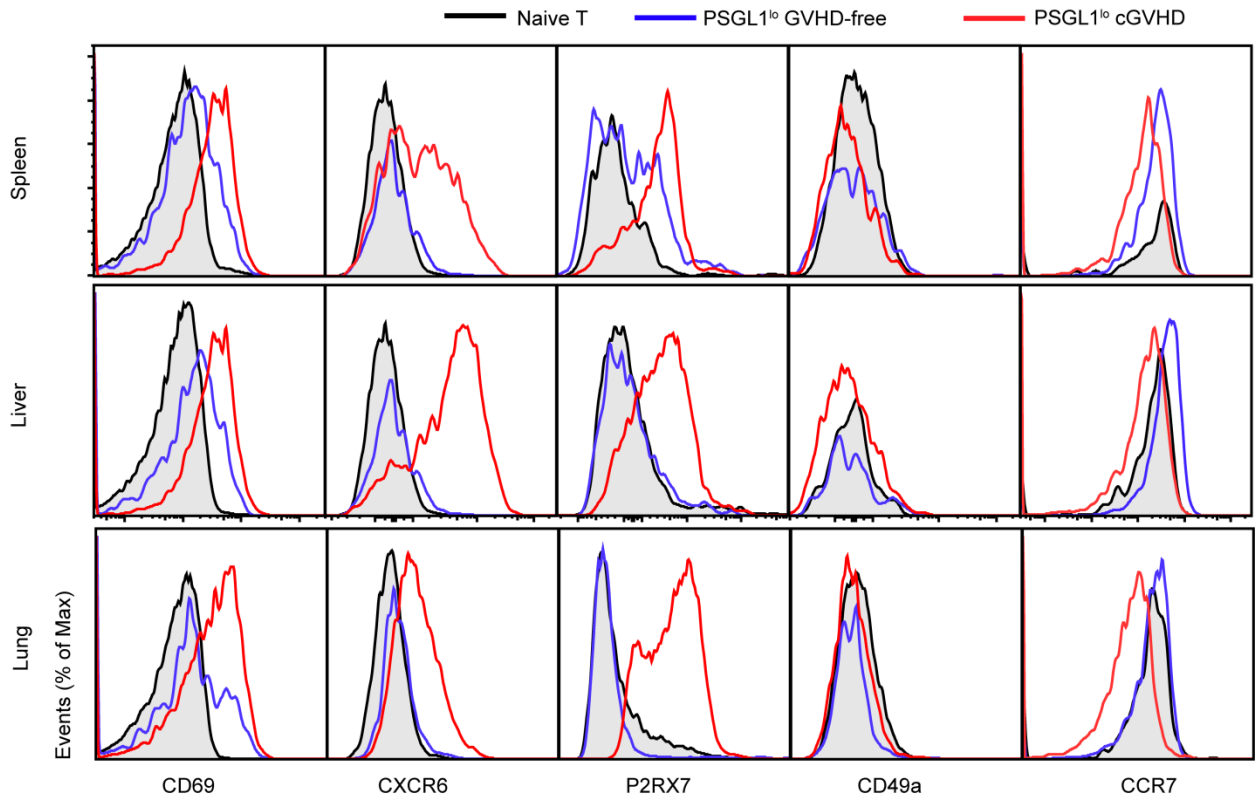

Supplemental Figure 5: PSGL1^{lo}CD4^{+} T cells are tissue resident T cells in cGVHD targeted tissues. Supplement to Figure 1D. Representative histograms showing surface expression of CD69, CXCR6, P2RX7, CD49a and CCR7 by naïve T cells and PSGL1^{lo}CD62L^{-} CD4^{+} T cells from the spleen, liver and lung of GVHD-free and cGVHD recipients. N=6-8, combined from at least 2 independent experiments.

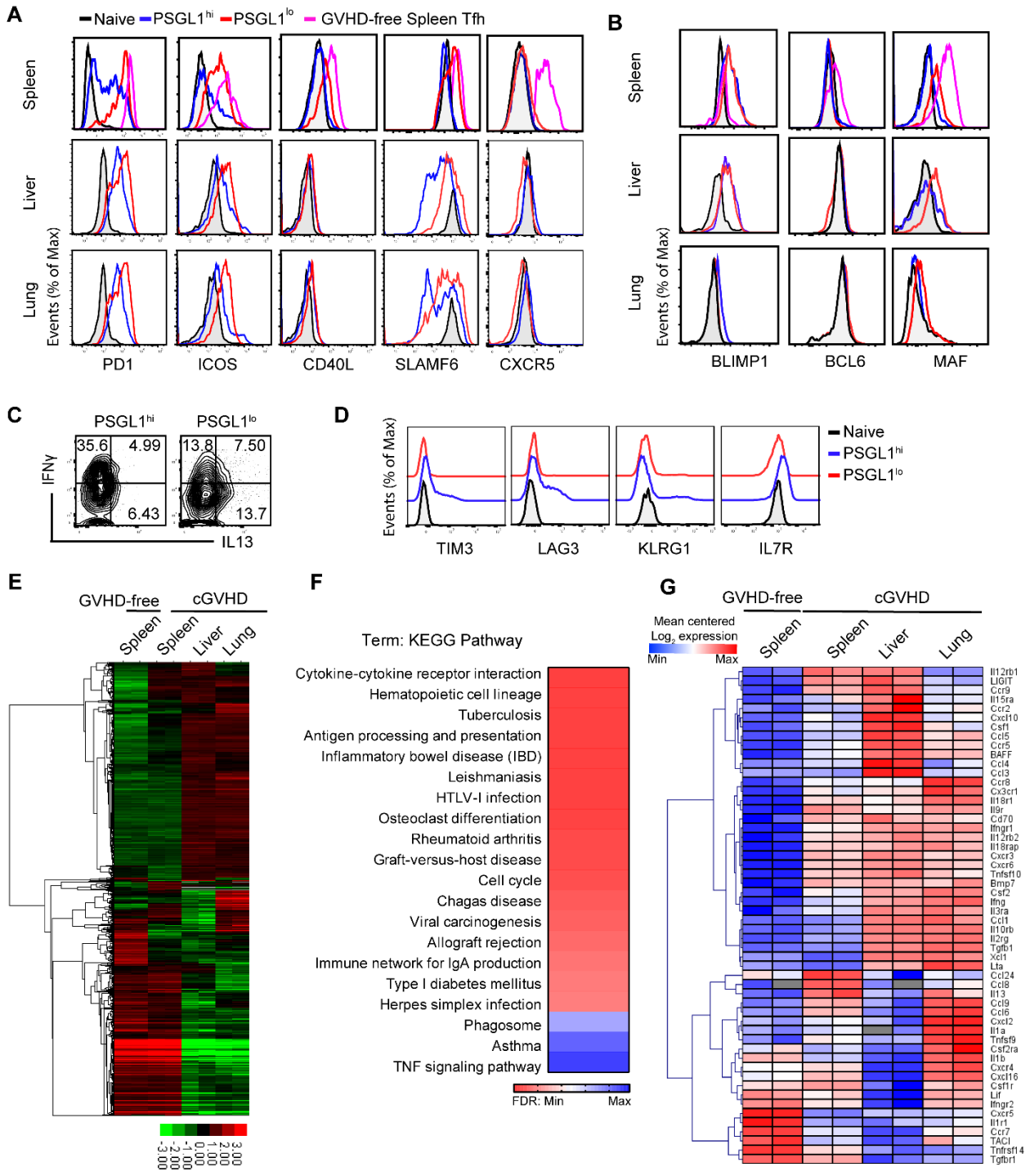

Supplemental Figure 6

Supplemental Figure 6: PSGL1^{lo}CD4^{+} T cells are B cell helpers. Panel A, B, C and D supplement Figure 3,D-G with representative flow cytometry patterns comparing naïve CD4^{+} T, and PSGL1^{hi} and PSGL1^{lo} CD62L^{-}CD4^{+} T cells from the spleen, liver and lung. **(A)** Representative histogram panels of PD1, ICOS, CD40L, SLAMF6 and CXCR5 expression. **(B)** Representative histogram panels of intracellular expression of BLIMP1, BCL6 and MAF. **(C)** Sorted PSGL1^{hi} and PSGL1^{lo} CD62L^{-}CD4^{+} T cells were stimulated with PMA and ionomycin and stained for intracellular IFNγ and IL13. **(D)** Representative flow cytometry histograms of surface expression of TIM3,LAG3, KLRG1 and IL7R. Panel E, F and G supplement the RNA-seq analysis. **(E)** Heatmap showed inter-organ PSGL1^{lo}CD4^{+}T cells comparison. **(F)** Predicted KEGG pathway of the upregulated genes in the PSGL1^{lo}CD4^{+}T cells derived from GVHD target liver and lung compared to the GVHD-free spleen PSGL1^{lo}CD4^{+}T cells. **(G)** Heatmap shows the genes related to the cytokine-cytokine receptor interaction from the KEGG pathway analysis.

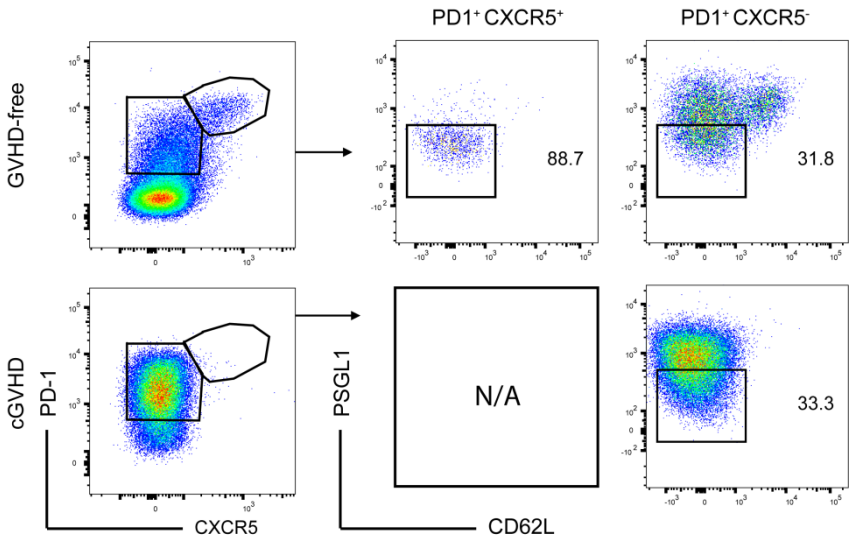

Supplemental Figure 7: PD1^{hi}CXCR5^{+} Tfh cells in the spleen of GVHD-free recipients are mostly PSGL1^{lo}CD4^{+} T cells. PD1^{+}CXCR5^{+} and PD1^{+}CXCR5^{-} CD4^{+} T cells from the spleen of GVHD-free and cGVHD mice are gated and shown CD62L versus PSGL1. One representative pattern is shown.

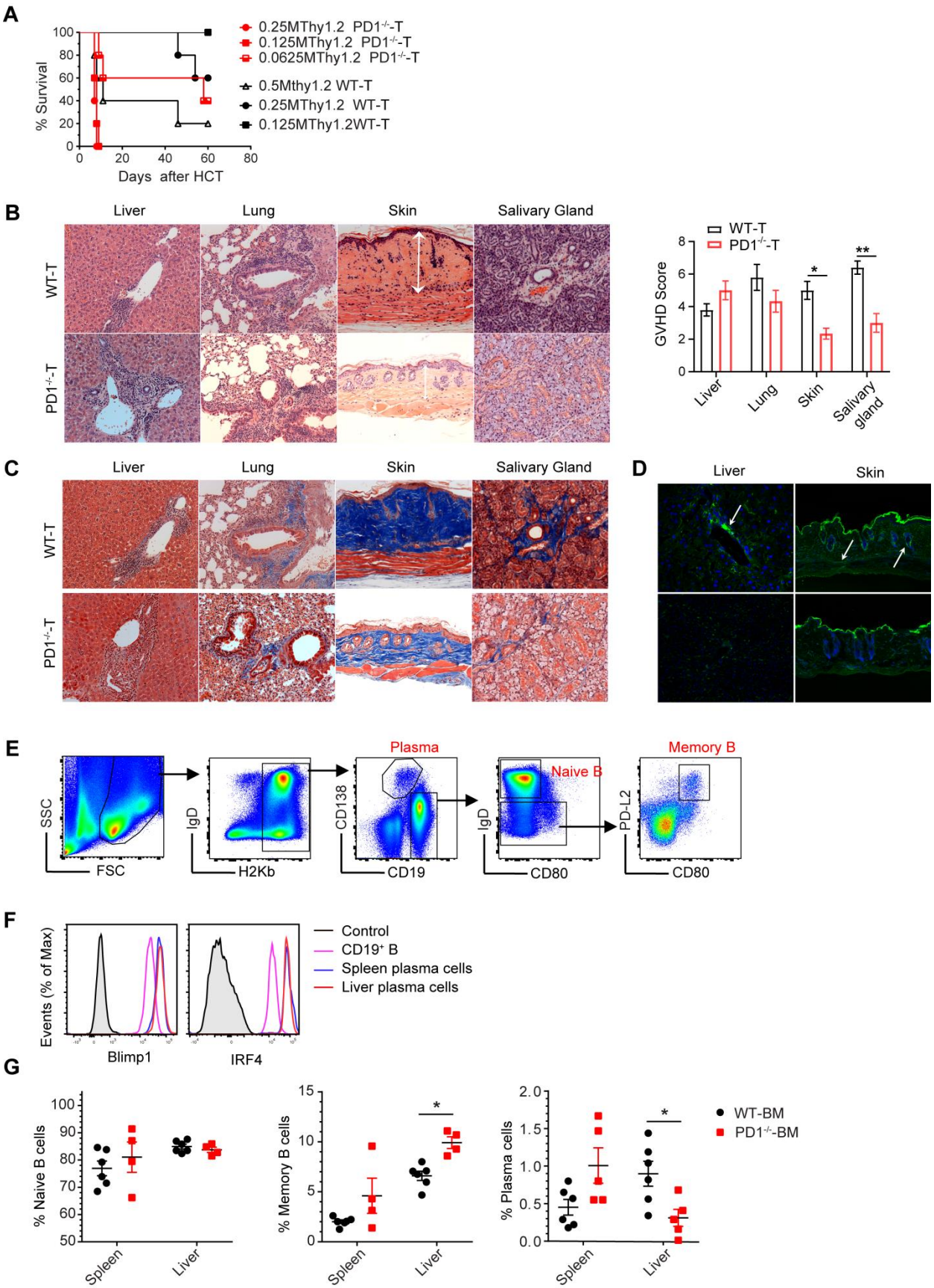

Supplemental Figure 8

Supplemental Figure 8: Impact of donor T cell PD1 deficiency on cGVHD pathogenesis.

This is a supplement to Figure 4, A-C**. (A)** Curves of %Survival of recipients given titrated numbers of WT or PD1$^{-/-}$ Thy1.2 T cells. N=10, combined from two replicate experiments. **(B)** Represented pathology feature of HE staining of liver, lung, skin and salivary glandv (original magnification, ×200). Scores were recorded as means ± SEM. **(C)** Representative micrographs of collagen deposition in the liver, lung, skin and salivary gland are shown from 1 of 3 replicates. (original magnification, ×200) **(D)** Representative micrographs of mouse IgG deposition in the liver and skin are shown from 1 of 3 replicates (original magnification, ×200). **(E)** Representative flow cytometry patterns for identifying naive B, memory B and plasma cells in the spleen and liver tissues of recipients given WT or PD1$^{-/-}$ donor T cells. **(F)** Intracellular staining of Blimp1 and IRF4 of CD19^{+} B, spleen and liver plasma cells. **(G)** Percentages of naïve, memory, and plasma cells in the spleen and liver of recipients given WT-TCD-BM or PD1$^{-/-}$-TCD-BM cells alone. Mean ± SEM is shown, N=4-6, combined from two replicate experiments. P values were calculated by one-way ANOVA. *p<0.05; **p<0.01; ***p<0.001; ****p<0.0001.

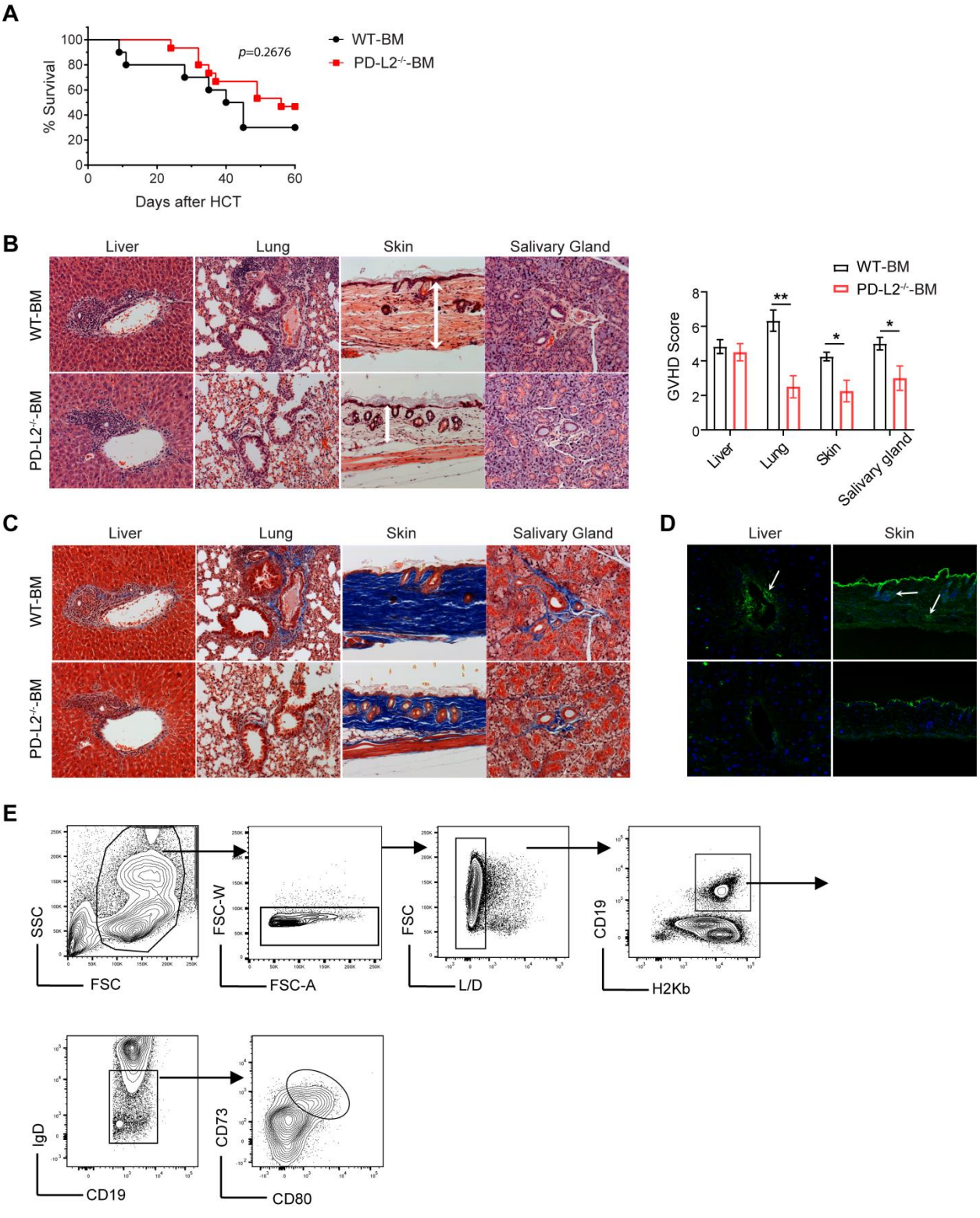

Supplemental Figure 9

Supplemental Figure 9: Comparison of cGVHD induction by WT and PD-L2$^{-/-}$ TCD-BM. This is a supplement to Figure 4, D-F. **(A)** Curves of % survival of recipients given WT and PD-L2$^{-/-}$ TCD-BM cells. N=10, combined from two replicate experiments. **(B)** Representative micrographs of pathology feature of HE staining of liver, lung, skin and salivary gland and means ± SEM of pathology score (original magnification, ×200). **(C)** Representative micrographs of collagen deposition in the liver, lung, skin and salivary gland are shown for 1 of 3 replicates (original magnification, ×200). **(D)** Representative micrographs of mouse IgG deposition in the liver and skin are shown for 1 of 3 replicates; the white arrows point to IgG deposition (original magnification, ×200). **(E)** Gating strategy for identifying CD80^{+}CD73^{+} memory B cells in recipients given WT or PD-L2$^{-/-}$ TCD-BM cells. P values were calculated by log-rank test **(A)** or one-way ANOVA **(B)**. *p<0.05; **p<0.01.

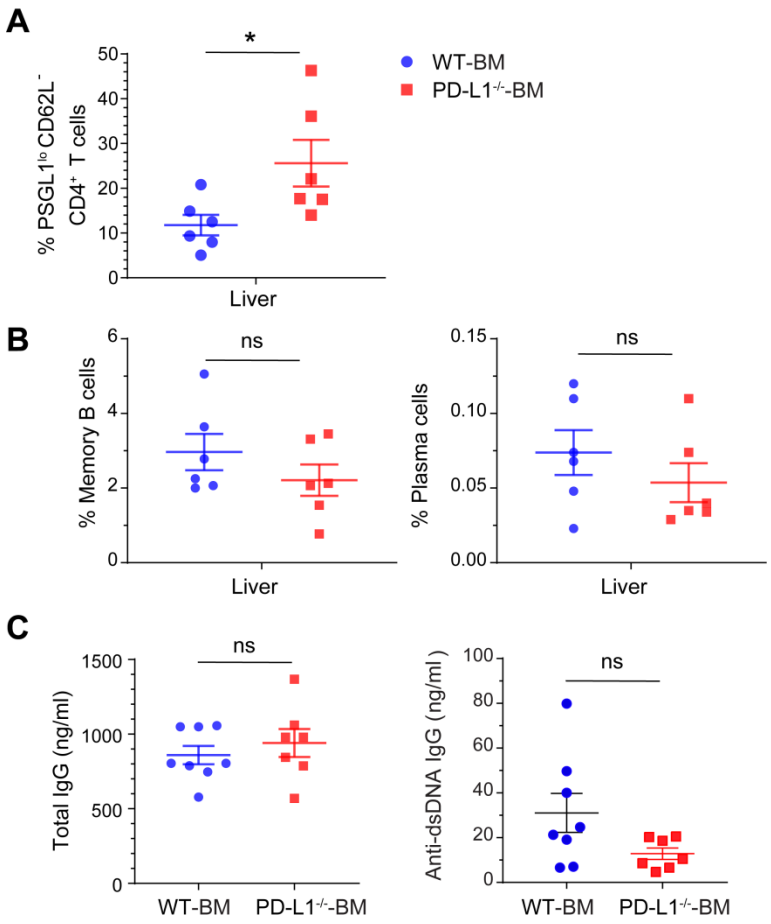

Supplemental Figure 10: PD-L1 deficiency on donor B cells does not significantly reduce total IgG or autoantibody production. Lethally irradiated BALB/c mice were given Thy1.2$^+$ T and WT- or PD-L1$^{-/-}$ -TCD-BM. 60 days after HCT, PSGL1^{lo}CD4$^+$ T cells, memory B cells and plasma cells in the liver tissue of the recipients were measured. **(A)** %PSGL1^{lo}CD62L$^-$CD4$^+$ T cells; **(B) %**memory B cells and %plasma cells; **(C)** Serum total IgG concentration and IgG anti-dsDNA autoantibody concentrations. Mean ± SEM is shown; N=6-8, combined at least 2 independent experiments. P values were calculated by unpaired 2-tailed Student's t-tests. *p<0.05.

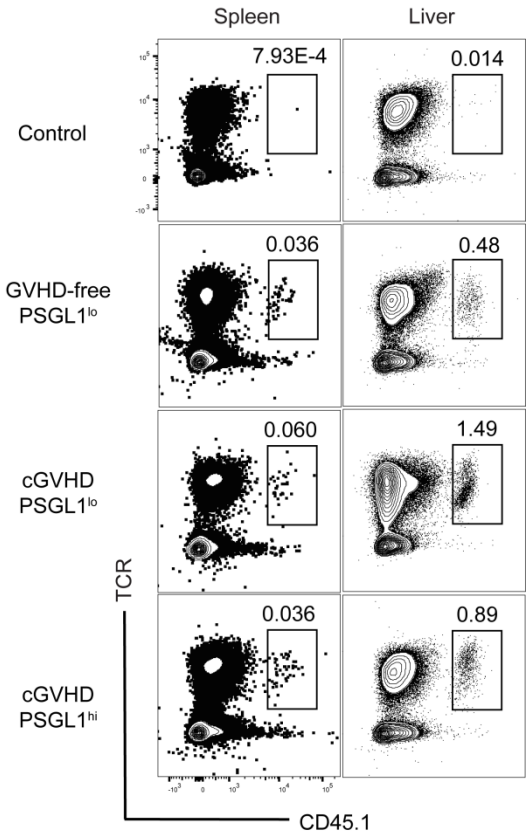

Supplemental Figure 11: Adoptively transferred PSGL1^{lo}CD4^{+} T cells from the liver and lung of cGVHD recipients preferentially appear in the recipient liver as compared to the spleen. This is a supplement to Figure 5B. Spleen and liver tissues of adoptive recipients given PSGL1^{lo} or PSGL1^{hi} CD4^{+} T cells were harvested at 14 days after cell transfer and measured for the percentage of the injected CD45.1^{+} T cells. A representative flow cytometry pattern is shown from 1 of 6-8 mice in each group.

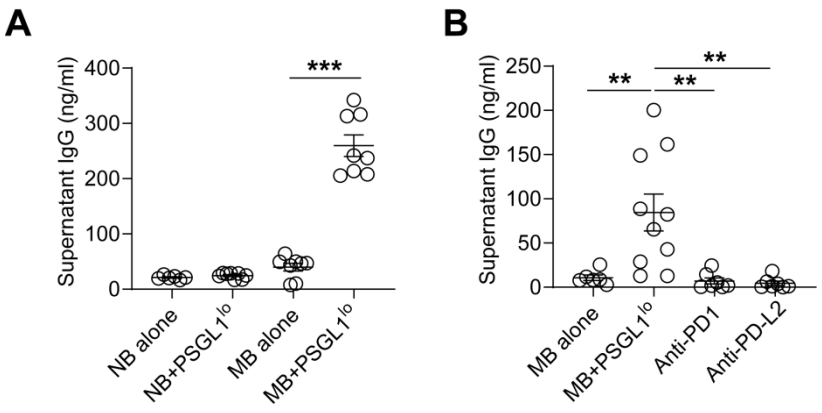

Supplemental Figure 12: PSGL1^{lo}CD4^{+} T cells augment IgG production by memory B cells in a PD1/PD-L2-dependent manner. Sorted PSGL1^{lo}CD4^{+} T cells from the liver and lung of cGVHD recipients were co-cultured with naïve B cells and memory B cells from the spleen of recipients given TCD-BM cells alone at a ratio of 1:5. **(A)** T cells were cultured with 5×10^4 B cells per well for 4 days. **(B)** T cells were cultured with 2×10^4 memory B cells per well for 4 days in the presence of 20μg/ml anti-PD1 or anti-PD-L2. Supernatants were measured for IgG concentration by ELISA. Data are presented as means ± SEM, combined from 3 replicate experiments. P values were calculated by one-way ANOVA (C). **p<0.01; ***p<0.001.

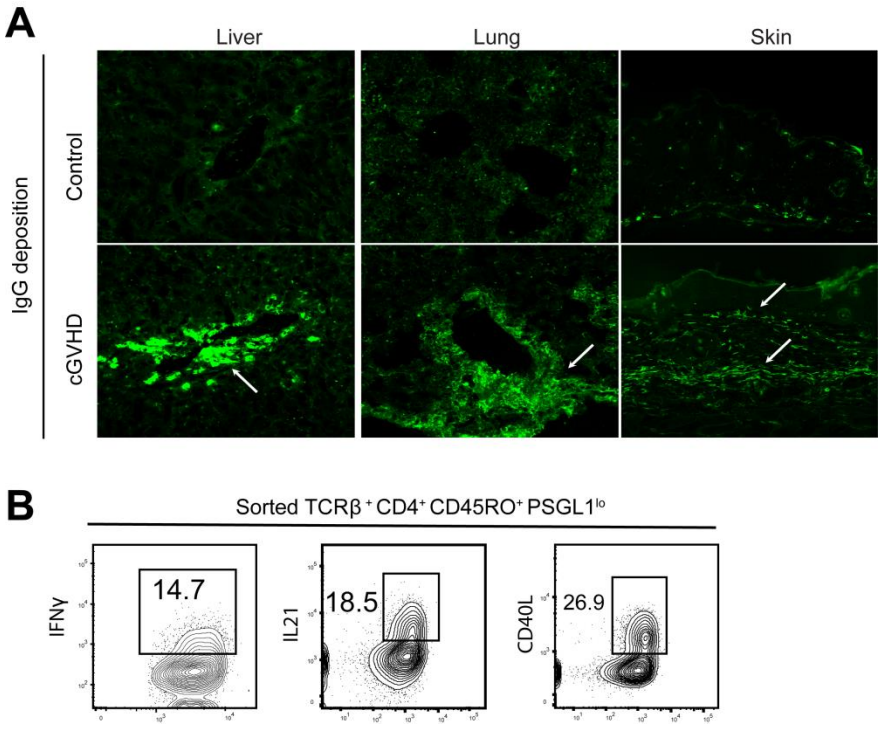

Supplemental Figure 13: Human IgG deposition in tissues of humanized mice with cGVHD. This is a supplement to Figure 8. **(A)** Represent micrograph of human IgG deposition in the liver, lung and skin is shown from 1 of 4 replicate experiments (original magnification, liver and lung,×200; skin,×100). The white arrows pointed at the IgG deposition. **(B)** Sorted liver $PSGL1^{lo}CD45RO^{+}CD4^{+}$ T cells were stimulated with PMA plus ionomycin and then stained with IFNγ, IL21 and CD40L. Representative flow cytometry pattern is shown from 1 of 2 replicate experiments.

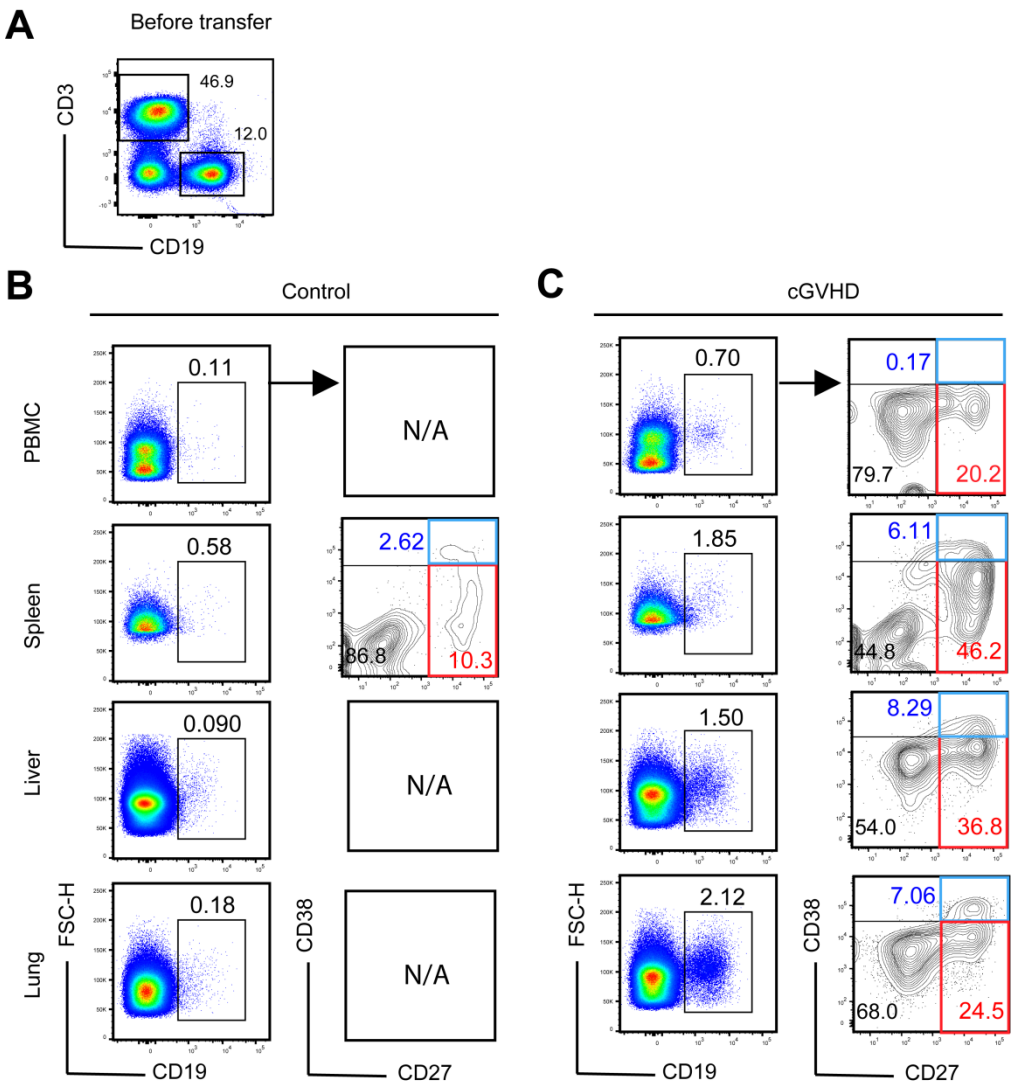

Supplemental Figure 14: Presence of B cell subsets in tissues of humanized mice with cGVHD. (A) A representative flow cytometry pattern of T and B cells in the healthy donor PBMC before transfer. **(B and C)** 60 days after transfer, $CD19^+$ B cells in the PBMC, spleen, liver and lung of $MHC^{-/-}$NSG control recipients and $MHC^{-/-}HLA\text{-}A2^+DR4^+$ NSG cGVHD recipients were gated and shown in CD27 versus CD38. Representative flow cytometry patterns are shown from 1 of 3 replicate experiments.

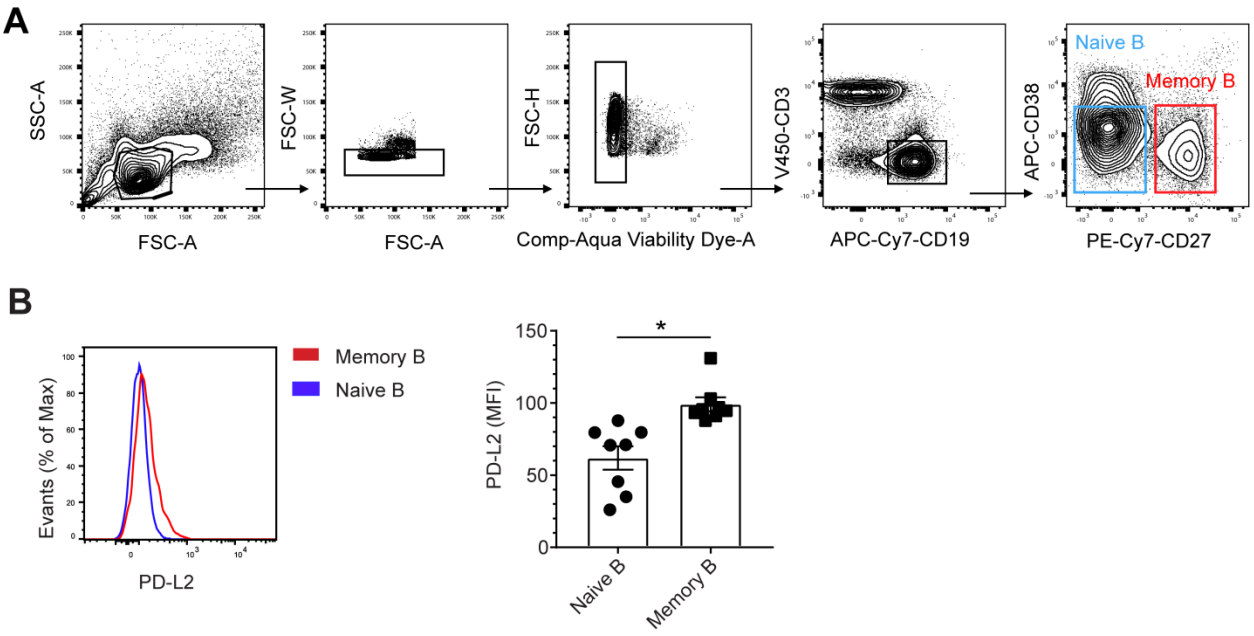

Supplemental Figure 15: Sorting strategy for naïve and memory human B cell subsets, and PD-L2 expression by memory B cells. **(A)** Representative flow cytometry sorting panels for naïve B cells ($CD3^{-}CD19^{+}CD27^{-}CD38^{lo/-}$) and memory B cells ($CD3^{-}CD19^{+}CD27^{+}CD38^{lo/-}$) from human PBMC. **(B)** Histograms of PD-L2 expression by gated naïve and memory B cells, and mean ± SEM of MFI is shown. N=8, combined from 2 independent experiments. P values were calculated by unpaired 2-tailed Student's t-tests. *p<0.05.

Supplemental Table 1. Clinical characteristics of GVHD patients

Number	Gender	Age	Disease	Donor Type	Graft Type	Conditioning	Immuno-suppression	GVHD Grade
1	Male	44	SAA	Allo unrelated	BM	TBI; CTX; ATG; FLUDARABINE	Tacrolimus; MTX	limited cGVHD
2	Male	73	AML	Allo unrelated	PBSC	Fludarabine; Melphalan	Tacrolinus; Sirolimus	Extensive cGVHD
3	Male	65	MDS	Allo related	PBSC	Fludarabine; Melphalan	Tacrolinus; Sirolimus	Extensive cGVHD
4	Male	66	other Acute leukemia	Allo unrelated	PBSC	Fludarabine; Melphalan	Tacrolinus; Sirolimus	Extensive cGVHD

Abbreviations: SAA, severe aplastic anemia; AML, acute myeloid leukemia; MDS, myelodysplastic syndrome; BM, bone marrow; PBSC, peripheral blood stem cells; TBI, total body irradiation; CTX, cyclophosphamide; ATG, antithymocyte globulin; MTX, methotrexate.

Supplemental Table 2. Characteristics of healthy volunteers

Number	Gender	Age
1	male	44
2	male	74
3	female	37
4	male	58
5	female	63
6	male	55
7	male	79

Supplemental Materials and Methods

Patients subjects.

Formalin-fixed liver biopsy tissue slides from unidentified chronic GVHD patients were provided by clinical pathology lab at Fred Hutchinson cancer center under an MTA between Fred Hutchison cancer center and City of Hope National Medical center. There are totally 5 patients.

Induction and assessment of GVHD:

For murine model of cGVHD, BALB/c recipient mice received 850 cGy total body irradiation (TBI) from a ^{137}Cs source. T cell-depleted bone marrow (TCD-BM), splenocytes, PBMC or sorted Thy1.2 cells from splenocytes of C57BL/6 donors were injected intravenously (i.v.) into recipients 8-10 hours later. For the humanized GVHD model, human PBMC (~25 million) containing 12 x 10^6 T cells from healthy donors were injected intraperitoneally (i.p.) into MHC-I$^{-/-}$ MHC-II$^{-/-}$ NSG mice and MHCI$^{-/-}$MHC-II$^{-/-}$HLA-A2^{+}DR4^{+} NSG mice. The assessment and scoring of clinical GVHD were monitored according to protocols described in our previous publications (1, 2).

Generation of MHC-I$^{-/-}$MHC-II$^{-/-}$ NSG and MHCI$^{-/-}$MHC-II$^{-/-}$HLA-A2^{+}DR4^{+} NSG mice:

1) MHC-I$^{-/-}$MHCII$^{-/-}$ NSG mice are generated by backcrossing NSG-Ab0 (Jax #021885) with NSG-β2M-KO (Jax #010636) as described in the diagram below.

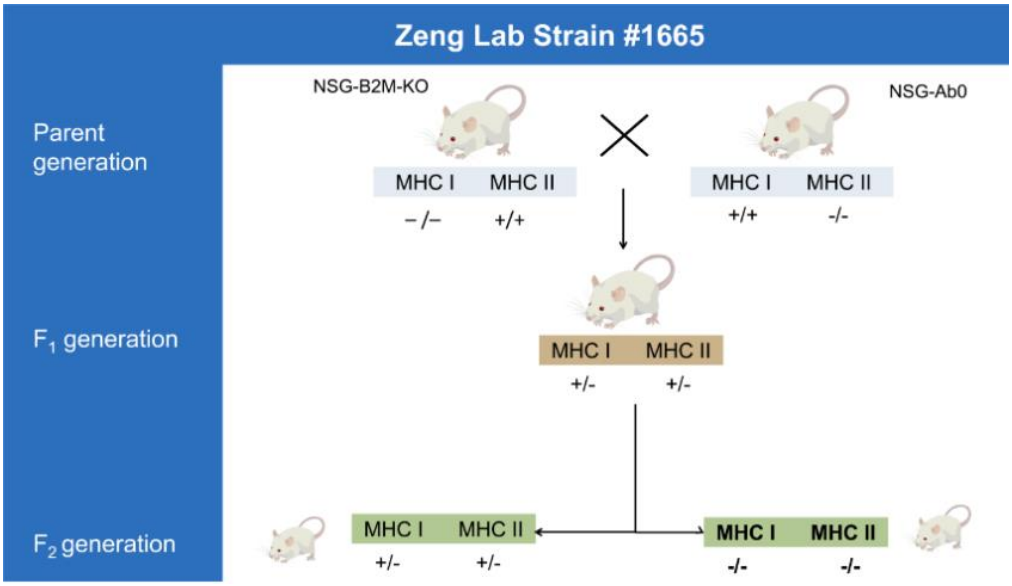

2) MHCI$^{-/-}$MHC-II$^{-/-}$HLA-A2^{+}DR4^{+} mice were generated by backcrossing NSG-HLA-A2 (Jax # 014570) and NSG-Ab0-DR4 (Jax #017637) with MHC-I$^{-/-}$ MHC-II$^{-/-}$ NSG mice (Zeng lab Strain #1665) as described in the diagram below.

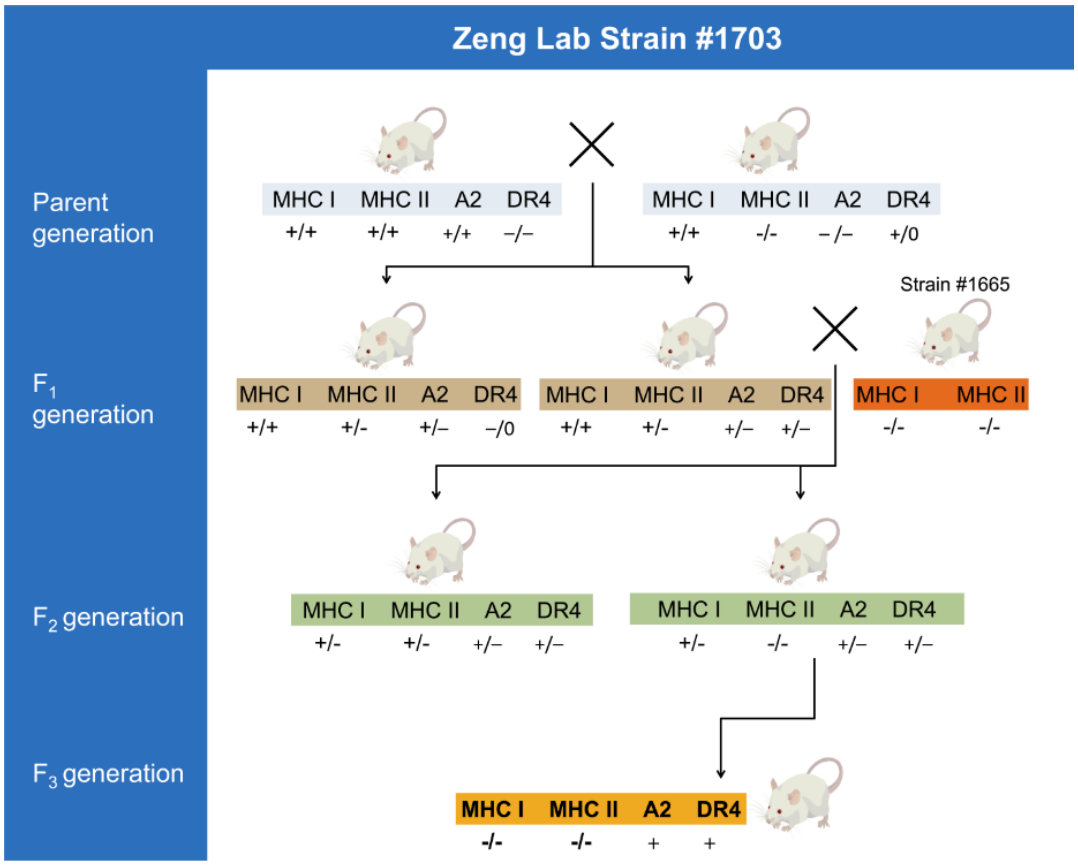

Mice were screened by PCR with primers below:

MHC-I primers: 5' TCT GGA CGA AGA GCA TCA GGG-3' ; 5'-TAT CAG TCT CAG TGG GGG TG-3'; 5'-CTG AGC TCT GTT TTC GTC TG-3'.

MHC-II primers: 5'-ATG GGC GAG TGC TAC TTC AC-3'; 5'- GCC CGC GTT CGC TCC AGG-3'; 5'- TCA ATG GCC GAT CCC ATA-3'.

HLA-A2 primers: 5'- CTT CAT CGC AGT GGG CTA C-3'; 5'- CGG TGA GTC TGT GAG TGG G-3'.

HLA-DR4 Primers: 5'- CCA CCA CTT CCT GCC TAC AT-3'; 5'- CCA GAC CGT CTC CTT CTT TG-3'.

Isolation of lymphocytes from GVHD target tissues

Thymus and spleen were harvested, minced and mashed through a cell strainer to make single cell suspension. Cells were washed twice for further procedures. For liver lymphocyte isolation, the minced liver was mashed through a cell strainer, and hepatic lymphocytes were further isolated with 70%-40% Percoll (Sigma-Aldrich) density gradient centrifugation at room temperature. For lung and skin lymphocyte isolation, tissues were cut into pieces and digested with Collagenase D (Sigma-Aldrich) and DNase (Sigma-Aldrich) I at 37^0C for 60 and 80 minutes, respectively. MNC were then isolated with Lympholyte-M (Cedarlane). Buffy coat cells were collected, washed twice and counted by a Cellometer Auto 2000 Cell Viability Counter (Nexcelom).

Antibodies, Flow Cytometry analysis and cell Sorting

The isolated cells were washed with cold 2%BSA PBS and blocked with anti-CD16/32(2.4G2, BIO-X CELL) for 10 minutes, then added surface antibodies staining for 15 minutes. The anti-murine antibodies included anti-CD4 (RM4-5,BD Bioscience), anti-CD3(17A2,Fisher Scientific),

anti-TCRβ(H57-597,Fisher Scientific), anti-H-2K^{b}(AF6-88.5,Fisher Scientific), anti-CD45.1 (A20, Fisher Scientific),anti-CD62L(MEL-14,Fisher Scientific), anti-PSGL1(2PH1,Fisher Scientific), anti-CD69 (H1.2F3, Fisher Scientific), anti-CXCR6 (DANID2,eBioscience), anti-P2RX7 (1F11, BD Pharmingen), anti-CCR7 (4B12, Fisher Scientific), anti-CD49a (HMα1,Biolegend), anti-CD127(A7R34,Fisher Scientific), anti-CD103 (2E7,Fisher Scientific), anti-PD1(29F.1A12, Biolegend), anti-ICOS (7E.17G9,Fisher Scientific), anti-CD40L(MR1,eBioscience), anti-SLAMF6 (13G3-19D,Fisher Scientific), anti-CXCR5 (SPRCL5,Fisher Scientific), anti-CD44 (IM7,Fisher Scientific), anti-CD19(1D3,Fisher Scientific), anti-CD138 (281-2,BD Bioscience), anti-IgD(IA6-2,Fisher Scientific), anti-IgM(RMM-1, ,Fisher Scientific), anti-CD38(#90,Fisher Scientific), anti-PD-L2(TY25,Fisher Scientific), anti-CD80(16-10A1,Fisher Scientific) and anti-CD73 (TY/11.8, Fisher Scientific) .

The anti-human antibodies included: anti-CD3(HIT3a,Biolegend), anti-CD4(A161A1, Biolegend), anti-CD45RO (UCHL1, Fisher Scientific), anti-CD45RA (HI100, Biolegend), anti-PSGL1(FLEG ,Fisher Scientific), anti-PD1(MIH4,Fisher Scientific), anti-ICOS(C398.4A, Biolegend),anti-CD154 (TRAP-1,BD Bioscience) anti-CCR7(150503,BD Bioscience), anti-CXCR5 (MU5UBEE,eBioscience), anti-TIGIT (VSTM3,Biolegend), anti-CD103(Ber-ACT8, Biolegend), anti-CD69(FN50.Biolegend), anti-CD19(HIB19,Fisher Scientific), anti-CD20(2H7,BD Bioscience), anti-CD27(M-T271,Biolegend), anti-CD38(HIT2,Biolegend), and anti-CD138 (44F9,Miltenyi Biotec), anti-IFN-γ (4S.B3, eBioscience) and anti-IL-21 (eBio3A3-N2, eBioscience).

Cells were washed in cold 2% BSA PBS, passed through a 70μm filter, and flow cytometry data were acquired on a BD Fortessa flow cytometer. Results were analyzed using FlowJo version 10 software.

For transcription factor analysis, cells were first stained with mixtures of antibodies against surface antigens and then fixed, permeabilized with a Foxp3/Transcription Factor Staining

Set(eBioscience), and stained with antibodies against Bcl6 (BCL-DWN, Fisher Scientific), Blimp1(5E7,BD Bioscience), Maf (sym0F1, Fisher Scientific). For intracellular cytokines analysis, cells of interest were first sorted to greater than 95% purity for $H2Kb^{+}$ $TCR\beta^{+}$ $CD4^{+}$ $CD62L^{-}$ $PSGL1^{lo}$ with a BD FACS ARIA SORP sorter at the City of Hope FACS facility. Sorted cells were then stimulated with PMA plus ionomycin and stained with IFN-γ (XMG1.2, Fisher Scientific), IL-13 (eBio13A, Fisher Scientific) and IL-21 (3A3-N2, eBioscience).

RNA sequencing analysis

RNA from equal numbers of sorted $H2Kb^{+}TCR\beta^{+}CD4^{+}CD62L^{-}PSGL1^{lo}$ cells and $H2Kb^{+}TCR\beta^{+}CD4^{+}CD62L^{-}PSGL1^{hi}$ cells was extracted with the RNeasy Mini Kit purchased from Qiagen. Total RNA sequencing was performed and analyzed by the Integrative Genomics Core, City of Hope National Medical Center (Duarte, CA).

For RNA sequencing, RNA concentration was measured by NanoDrop 1000 (Thermo Fisher Scientific, Waltham, MA), and RNA integrity was determined with the use of a 2100 Bioanalyzer (Agilent Technologies, Santa Clara, CA). Libraries were constructed from 300 ng total RNA for each sample by using KAPA Stranded mRNA-Seq Kit (Kapa Biosystems, Wilmington, MA) with 10 cycles of PCR amplification. Libraries were purified using AxyPrep Mag PCR Clean-up kit (Thermo Fisher Scientific). Each library was quantified by using a Qubit fluorometer (Life Technologies), and the size distribution was assessed by using a 2100 Bioanalyzer (Agilent). Cluster generation was done according to the TruSeq SR Cluster Kit V4-cBot-HS (Illumina), and sequencing was performed on an Illumina® Hiseq 2500 (Illumina, San Diego, CA, USA) instrument to generate 51 bp single-end reads. Quality control of RNA-Seq reads was performed using FastQC.

Histopathology

Skin, lung, liver and salivary gland from GVHD-free or cGVHD mice were harvested and fixed in 10% neutral formalin and processed in paraffin blocks. The tissues embedded paraffin blocks were cut into 5 μm section and stained with hematoxylin and eosin (HE) and Masson's Trichrome by the Pathology Solid Tumor Core at the City of Hope.

Immunofluorescence Staining

For IgG deposition in liver, lung, skin, salivary gland and thymus, cryosections were stained with Alexa Fluro 488-labeled goat anti-mouse IgG for mouse and FITC-labeled rabbit anti-human IgG for humanized samples according to previous publications of our group (1, 2). For liver T and B staining, liver cryosections were stained with rabbit anti-mouse CD4 (ERP19514, Abcam), rat anti-mouse CD162 (4RA10, BD Pharmingen) and Biotin rat anti-mouse B220 (RA3-6B2, BD Pharmingen), CD273 polyclonal antibody (Invitrogen). Images were acquired on a Confocal Zeiss LSM700 microscope at 200X magnification.

Immunohistochemistry staining

Triple IHC stains were performed on Ventana Discovery Ultra (Ventana Medical Systems, Roche Diagnostics, Indianapolis, USA) IHC automated stainer.

Briefly, tissue samples were sectioned at a thickness of 5 μm and put on positively charged glass slides. The slides were loaded on the machine, deparaffinized and rehydrated, followed by endogenous peroxidase activity inhibition and antigen retrieval. Then, the three antigens were sequentially detected and heat inactivation was used to prevent antibody cross-reactivity between the same species. Following each primary antibody incubation, DISCOVERY anti-Rabbit HQ or NP or DISCOVERY anti-Mouse HQ or NP and DISCOVERY anti-HQ-HRP or anti-NP-AP were incubated.The stains were then visualized with DISCOVERY Yellow Kit,

DISCOVERY Teal Kit and DISCOVERY Purple Kit, respectively, counterstained with hematoxylin (Ventana) and coverslipped. The antibodies used were: Rabbit anti-human CD3 (2GV6,Ventana, Roche Diagnostics), Rabbit anti-human CD4 (SP35,Ventana, Roche Diagnostics), Rabbit anti-human CD20 (L26,Ventana, Roche Diagnostics), Rabbit anti-human PAX5(SP34,Ventana, Roche Diagnostics),anti-human Maf(EPR16484,Abcam), anti-human PSGL1(# 688124,R&D). Murine liver and lung samples were also stained with anti-mouse B220 (RA3-5B2, BD Biosciences), anti-mouse CD3 (2GV6,Ventana, Roche Diagnostics) and anti-mouse CD4 mAbs(D7D2Z, Cell Signaling Technology) by the Pathology Solid Tumor Core at the City of Hope. Slides were imaged at 200x magnification with Zeiss Observer II.

Total IgG and Autoantibodies detection

Serum samples from GVHD mice and control mice were collected and used for measuring IgG concentration. For measuring total IgG, the high-binding 96-well plate was first coated with purified anti-mouse IgG overnight and then washed with 0.5% Tween 20 PBS. Serum samples were later added and incubated for 2 hours at room temperature.The plate was washed 4 times, and the secondary antibody goat anti-mouse IgG HRP was further added for 30 minutes. Plate was washed and TMB solution was added to measure the Ig concentration by a Tecscan machine. For measuring IgG anti-dsDNA autoantibodies, commercial mouse or human anti-dsDNA ELISA kit (Signosis, Santa Clara) was applied. For measuring human IgG concentration, we used the Human IgG ELISA ready-SET-Go Kit (Invitrogen).

Cell transfer experiments

Chronic GVHD was induced by transplanting TCD-BM cells ($2.5x10^6$) and splenocytes ($1x10^6$) from CD45.1$^+$-congenic C57BL/6 donors into lethally irradiated BALB/c recipients. At 30 days after HCT, cells isolated from spleen, liver, and lung were stained with anti-H-2K^b, anti-CD3, anti-CD4, anti-CD62L, anti-PSGL1 and then sorted by ARIA SORP. Sorted H2Kb$^+$CD62L$^-$

PSGl1^{lo}CD4^{+}T cells were transferred to GVHD-free adoptive recipients at 14 days after HCT with CD45.2^{+} TCD-BM (2.5x10^{6}). 14 days after cell transfer, MNC from the spleen and liver were analyzed for percentage and yield of PSGL1^{lo}CD4^{+} T cells, memory B and plasma cells. At the same time, serum was collected for measuring total IgG and IgG anti-dsDNA antibodies.

In vivo Anti-IL6R antibody blocking

Recipient animals were given 500μg Anti-mouse IL6R antibody (#15A7, BioXcell) and control Rat IgG per mice at day -1 and day 0 and then treated weekly by intraperitoneal injection.

T-B cell co-cultures

60 days after transfer of HLA-A2^{-}DR4^{-} human PBMC into MHC$^{-/-}$HLA-A2^{+}DR4^{+} NSG mice, cells were isolated from the spleen, liver and lung. Human CD4^{+} T cells were enriched by magnetic beads selection (Miltenyi) and then sorted with flow cytometry for CD45RO^{+}PSGL1^{lo}CD4^{+} T cells. Autologous naïve B cells (CD3^{-}CD19^{+}CD38$^{lo/-}$CD27^{-}) and memory B cells (CD3^{-}CD19^{+}CD38^{-}CD27^{+}) from cryopreserved samples were sorted by an ARIA SORP. Sorted T cells and memory B cells were mixed in a 1:10 ratio in RPMI 1640/10% FBS culture medium and stimulated with lipopolysaccharide (LPS, Sigma-Aldrich) and highly purified staphylococcal enterotoxin B (SEB,Toxin Technology.Inc) for 7 days as indicated (3). Cells were harvested for enumeration of plasma cells defined as CD19^{+}CD20^{lo}CD27^{+}CD138^{+} by BD Fortessa. Supernatants were collected for measuring total IgG by ELISA (Invitrogen). For functional blocking assays, 20 μg/ml IL-21R Fc (R&D Systems), 10 μg/ml anti-PD1 (J116, BIO-X CELL) and 10 μg/ml anti-PD-L2 (R&D Systems) were added to cultures.

For murine T/B cell cocultures, donor derived H2Kb^{+}PSGL1^{lo}CD62L^{-}TCRβ^{+}CD4^{+}T cells were cultured with naïve B cells (CD19^{+}IgD^{+}CD80^{-}) or memory B cells (CD19^{+}IgD^{-}CD80^{+}PD-L2^{+}) from GVHD-free spleen for 4 days in a 1:5 ratio with 5×10^{4} or 2×10^{4} B cells per well, and

supernatants were collected for measuring total IgG level. For blocking assays, 20 μg/ml anti-mouse PD1 (29F.1A12) or 20 μg/ml anti-mouse PD-L2 (TY25) were added.

Reference

1. Jin H, Ni X, Deng R, Song Q, Young J, Cassady K, Zhang M, Forman S, Martin PJ, Liu Q, et al. Antibodies from donor B cells perpetuate cutaneous chronic graft-versus-host disease in mice. *Blood.* 2016;127(18):2249-60.
2. Deng R, Hurtz C, Song Q, Yue C, Xiao G, Yu H, Wu X, Muschen M, Forman S, Martin PJ, et al. Extrafollicular CD4(+) T-B interactions are sufficient for inducing autoimmune-like chronic graft-versus-host disease. *Nat Commun.* 2017;8(1):978.
3. Rao DA, Gurish MF, Marshall JL, Slowikowski K, Fonseka CY, Liu Y, Donlin LT, Henderson LA, Wei K, Mizoguchi F, et al. Pathologically expanded peripheral T helper cell subset drives B cells in rheumatoid arthritis. *Nature.* 2017;542(7639):110-4.